

Alteration of Nucleic Acid Structure and Stability Modulates the Efficiency of Minus-Strand Transfer Mediated by the HIV-1 Nucleocapsid Protein*

Received for publication, February 13, 2004, and in revised form, July 21, 2004
Published, JBC Papers in Press, July 22, 2004, DOI 10.1074/jbc.M401646200

Susan L. Heilman-Miller, Tiyun Wu, and Judith G. Levin‡

From the Laboratory of Molecular Genetics, NICHD, National Institutes of Health, Bethesda, Maryland 20892-2780

During human immunodeficiency virus type 1 minus-strand transfer, the nucleocapsid protein (NC) facilitates annealing of the complementary repeat regions at the 3'-ends of acceptor RNA and minus-strand strong-stop DNA ((-) SSDNA). In addition, NC destabilizes the highly structured complementary trans-activation response element (TAR) stem-loop (TAR DNA) at the 3'-end of (-) SSDNA and inhibits TAR-induced self-priming, a dead-end reaction that competes with minus-strand transfer. To investigate the relationship between nucleic acid secondary structure and NC function, a series of truncated (-) SSDNA and acceptor RNA constructs were used to assay minus-strand transfer and self-priming *in vitro*. The results were correlated with extensive enzymatic probing and *mFold* analysis. As the length of (-) SSDNA was decreased, self-priming increased and was highest when the DNA contained little more than TAR DNA, even if NC and acceptor were both present; in contrast, truncations within TAR DNA led to a striking reduction or elimination of self-priming. However, destabilization of TAR DNA was not sufficient for successful strand transfer: the stability of acceptor RNA was also crucial, and little or no strand transfer occurred if the RNA was highly stable. Significantly, NC may not be required for *in vitro* strand transfer if (-) SSDNA and acceptor RNA are small, relatively unstructured molecules with low thermodynamic stabilities. Collectively, these findings demonstrate that for efficient NC-mediated minus-strand transfer, a delicate thermodynamic balance between the RNA and DNA reactants must be maintained.

Reverse transcription consists of a complex series of reactions catalyzed by the virion-associated enzyme reverse transcriptase (RT)¹ that lead to conversion of the single-stranded RNA genome into an integration-competent linear double-stranded DNA (1). This process is facilitated by host and viral accessory proteins, one of which is the viral nucleocapsid protein (NC). Human immunodeficiency virus type 1 (HIV-1) NC is a small, highly basic, nucleic acid-binding protein with two zinc fingers, each containing the invariant CCHC metal ion-binding

motif (2–5). NC functions as a nucleic acid chaperone in an ATP-independent manner (6) and catalyzes nucleic acid conformational rearrangements that lead to the formation of the most thermodynamically stable structure (Ref. 7 and reviewed in Refs. 8–11). This activity is required for efficient reverse transcription and allows NC to promote intermolecular annealing of nucleic acids with significant stretches of base complementarity (7, 12–26), destabilization of secondary structures in RNA and DNA templates that are responsible for RT pausing (27–30), unwinding of primer tRNA (19, 31–34), primer placement (12, 15, 19, 32, 33, 35–38), and the initiation step (39–41).

NC nucleic acid chaperone activity is also critical for the minus-strand (reviewed in Refs. 8, 10, and 11) and plus-strand (18, 20, 22, 42) transfer events that are required to complete elongation of minus- and plus-strand DNAs and to generate the long terminal repeats that flank the ends of proviral DNA (43). During HIV-1 minus-strand transfer, minus-strand strong-stop DNA ((-) SSDNA), the first product of reverse transcription, is translocated to the 3'-end of viral RNA in a reaction mediated by base pairing of the 97-nucleotide (nt) complementary repeat (R) regions present at the 3'-ends of the RNA and DNA molecules (1). Recent reports from Bambara and co-workers (44, 45) indicate that a major pathway for minus-strand transfer involves an acceptor-initiated strand invasion mechanism that allows strand transfer to occur at sites within the R region, with a smaller contribution from end terminal transfer. In addition to stimulating minus-strand transfer (21, 23, 25, 30, 44–56), NC also inhibits a competing self-priming reaction induced by the complementary trans-activation response element (TAR) DNA structure in (-) SSDNA (21, 23, 25, 51, 53, 55–59).

Self-priming occurs when intramolecular fold-back structures formed at the 3'-end of (-) SSDNA are extended by RT to produce minus-strand DNAs with plus-strand DNA extensions (25, 51, 56, 58, 59); these products are termed “self-priming products” (SP products or SP DNAs). In the absence of acceptor RNA, NC alone has little or no effect on HIV-1 (-) SSDNA self-priming (25, 56, 59). Driscoll and Hughes (56) and Golinelli and Hughes (59) have also reported that under conditions where acceptor RNA is omitted, self-priming is effectively blocked only if NC is added together with a 70-fold excess of short DNA oligonucleotides complementary to the 3'-end of (-) SSDNA. These short DNAs mimic the small RNA fragments produced by degradation of genomic RNA during minus-strand DNA synthesis (56, 58, 59).

Fluorescence and absorbance spectroscopy studies have provided physical evidence indicating that the TAR DNA stem-loop is quite stable (25, 60–62). Addition of NC to TAR DNA causes “fraying” of the terminal base pairs of the stem-loop, which alters the conformational equilibrium of the DNA in favor of less stable structures (25, 60–63). The fact that modest changes in the conformational state of DNA molecules in the

* The costs of publication of this article were defrayed in part by the payment of page charges. This article must therefore be hereby marked “advertisement” in accordance with 18 U.S.C. Section 1734 solely to indicate this fact.

‡ To whom correspondence should be addressed: Lab. of Molecular Genetics, NICHD, NIH, Bldg. 6B, Rm. 216, Bethesda, MD 20892-2780. Tel.: 301-496-1970; Fax: 301-496-0243; E-mail: levinju@mail.nih.gov.

¹ The abbreviations used are: RT, reverse transcriptase; NC, nucleocapsid protein; HIV-1, human immunodeficiency virus type 1; (-) SSDNA, minus-strand strong-stop DNA; nt, nucleotide(s); R, repeat; SP, self-priming; MNase, micrococcal nuclease; TAR, trans-activation response element.

TAR DNA population are not reflected in biochemical assays for self-priming (25, 56, 59) could be due to the low sensitivity of these assays or to the possibility (25) that partial melting of the TAR DNA stem-loop is not sufficient to inhibit self-priming. However, when NC and acceptor RNA are *both* present, there is a dramatic shift in the majority of the TAR DNA molecules to an unfolded state, which blocks self-priming and enables successful strand transfer to occur (25). Interestingly, *in vitro* studies with mutant HIV-1 NC proteins have demonstrated that the zinc finger motifs are required for NC-dependent inhibition of self-priming and destabilization of highly structured nucleic acids (21, 23, 64–67), including the TAR stem-loops in (–) SSDNA (HIV-1 (21, 23, 60) and feline immunodeficiency virus (68)) and in viral RNA (69).

In this work, we have examined the effect of nucleic acid secondary structure upon the ability of NC to stimulate efficient minus-strand transfer and have focused on structural determinants in both (–) SSDNA and acceptor RNA. Our approach was to test a series of truncated (–) SSDNA and acceptor RNA constructs using an *in vitro* assay that mimics the biologically relevant events of minus-strand transfer. The results of these assays are interpreted in terms of nucleic acid stability as judged by enzymatic probing and *mFold* analysis of individual (–) SSDNA or acceptor RNA constructs. Surprisingly, we found that destabilization of (–) SSDNA alone and elimination of self-priming by disruption of the TAR DNA stem-loop did not necessarily result in an increase in strand transfer: destabilization of acceptor RNA structure was also required. Thus, NC mediates efficient strand transfer only if both (–) SSDNA and acceptor RNA are moderately structured. Collectively, these results demonstrate that a delicate balance must exist between the stabilities of intramolecular secondary structures in (–) SSDNA and acceptor RNA and the stability of the intermolecular strand transfer duplex.

EXPERIMENTAL PROCEDURES

Proteins—HIV-1 RT was obtained from Worthington. Micrococcal nuclease (MNase) was purchased from U. S. Biochemical Corp. (Cleveland, OH). The following enzymes were obtained from Ambion Inc. (Austin, TX): DNase I, RNase T1, RNase A, RNase V1, S1 nuclease, and proteinase K. *Taq* DNA polymerase was obtained from Roche Applied Science. Wild-type HIV-1 NC was a generous gift from Dr. Robert Gorelick (SAIC Frederick, Inc., NCI-Frederick, Frederick, MD). The protein was prepared as described previously (28).

Plasmids and Synthetic (–) SSDNAs—Plasmid pJA has been described previously (51); it contains the 3′-half of HIV-1 pNL4-3 DNA (70), starting from the EcoRI site at nt 5743 and including all of U5. This plasmid was used for preparation of the 148-nt acceptor RNA by linearizing the DNA with FspI (New England Biolabs Inc., Beverly, MA). Linearized DNA was purified by extracting with 1:1 (v/v) phenol/chloroform, precipitating with ethanol, and resuspending in diethyl pyrocarbonate-treated water to a final concentration of 1 $\mu\text{g}/\mu\text{l}$. Synthetic (–) SSDNAs of varying lengths were obtained from Integrated DNA Technologies (Coralville, IA). The DNAs were purified by the company by PAGE and resuspended in diethyl pyrocarbonate-treated water prior to use.

PCR Amplification of Transcription Templates—DNA templates for transcription of acceptor RNA truncation mutants were prepared by PCR amplification of pJA (51). In all cases, the upstream primer included a T7 promoter, whereas the downstream primer defined the 3′-end of the RNA transcript. PCR primers were obtained from either Lofstrand Laboratories Ltd. (Gaithersburg, MD) or Integrated DNA Technologies. The sequences for the upstream primers were as follows: for RNAs 117, 104, and 84, 5′-TAA TAC GAC TCA CTA TAG GGA GTG GCG AGC CCT GAC; for RNAs 100, 87, and 67, 5′-TAA TAC GAC TCA CTA TAG GAT GCT GCA TAT AAG CAG CTG; and for RNAs 70 and 50, 5′-TAA TAC GAC TCA CTA TAG GCT GCT TTT TGC CTG TAC TGG. The sequences for the downstream primers were as follows: for RNAs 117 and 100, 5′-CAG TGG GTT CCC TAG TTA; for RNAs 104, 87, and 70, 5′-AGT TAG CCA GAG AGC TCC CAG; and for RNAs 84, 67, and 50, 5′-GGC TCA GAT CTG GTC. RNAs 100, 87, 70, 67, and 50 all contained an additional G at their 5′-end to facilitate transcription by

T7 RNA polymerase (71). PCRs were performed with *Taq* DNA polymerase, and the products were purified with commercial kits (Promega or Amersham Biosciences). The purified DNA was resuspended in diethyl pyrocarbonate-treated water to a final concentration of 0.5–1 $\mu\text{g}/\mu\text{l}$.

RNA Preparation—RNAs were transcribed *in vitro* using the T7-MEGAscript kit (Ambion Inc.) following the protocol supplied by the manufacturer. Following incubation, the transcription products were precipitated with ethanol, and unincorporated ribonucleoside triphosphates were removed by purification over a Chromaspin-30 column (Clontech) or by denaturing PAGE on a 6% gel.

In Vitro Minus-Strand Transfer Assay—The *in vitro* strand transfer assay has been described previously (25, 51). Briefly, synthetic (–) SSDNAs (0.2 pmol; final concentration of 10 nM) labeled at their 5′-ends with ^{32}P (72) were incubated with reaction buffer containing 50 mM Tris-HCl (pH 8.0), 75 mM KCl, 1 mM dithiothreitol, 0.1 mM dNTPs, and 7 mM MgCl_2 in a final volume of 20 μl . Where specified, 0.2 pmol of acceptor RNA (final concentration of 10 nM) and HIV-1 NC (at a ratio of one NC molecule to 0.9 nt of nucleic acid) were also added to the reaction mixture. Reactions were initiated by addition of HIV-1 RT (0.2 pmol; final concentration of 10 nM). Following incubation at 37 °C for 30 min, reactions were terminated by addition of EDTA (final concentration of 50 mM) and proteinase K (final concentration of 0.5 $\mu\text{g}/\mu\text{l}$), followed by heating to 65 °C for 15 min and extraction with 1:1 (v/v) phenol/chloroform. The aqueous phase was mixed with 8 μl of formamide loading buffer (U. S. Biochemical Corp.) and heated to 95 °C for 3 min, and a 5- μl aliquot of the mixture was subjected to denaturing PAGE on either a 6 or 8% gel. DNA products were visualized and quantified using a PhosphorImager (Amersham Biosciences) and ImageQuant software as described previously (51). The amounts of SP and transfer products formed are expressed as nanomolar. To express these amounts as percent of total substrate, the nanomolar values should be multiplied by 10. Note that in this study, the 128-nt (–) SSDNA and 148-nt acceptor RNA were each designated as “full-length.”

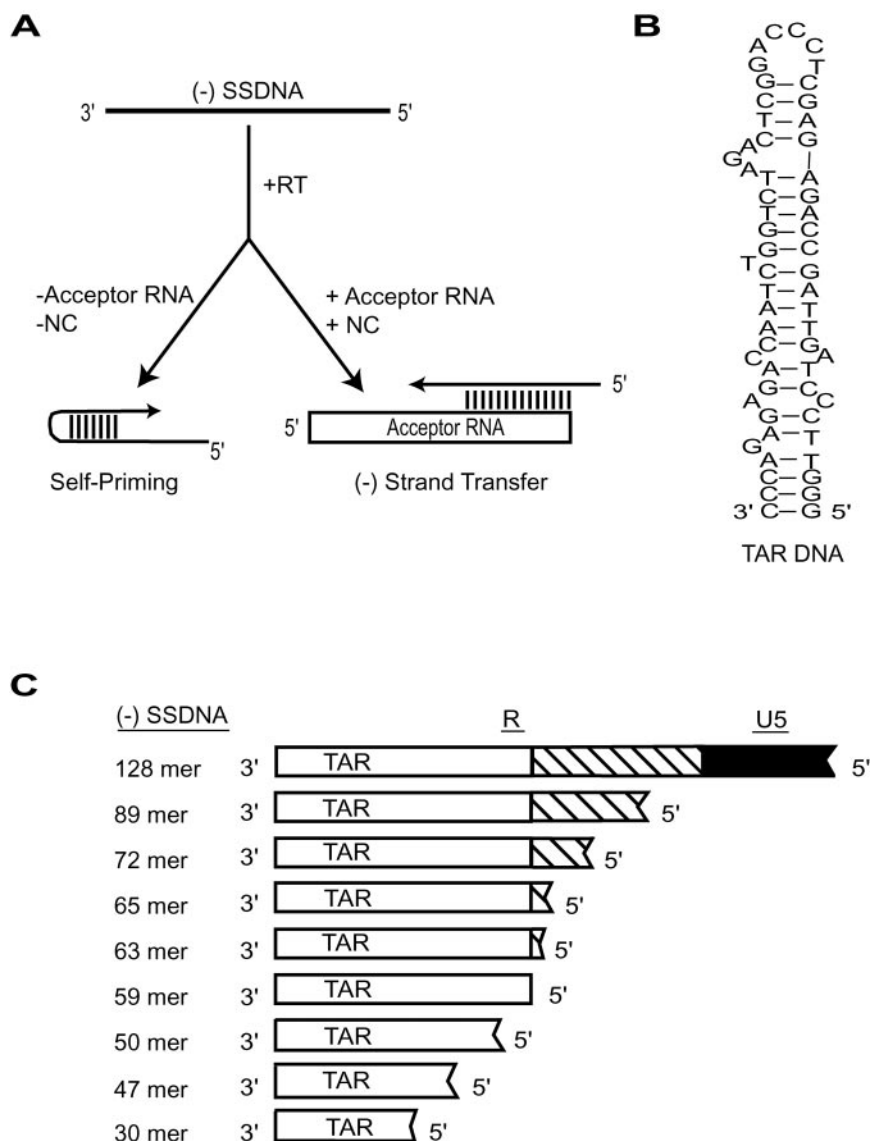
Enzymatic Mapping of (–) SSDNAs—5′- ^{32}P -Labeled synthetic (–) SSDNAs (~5 nM) were mixed in DNase I buffer (10 mM Tris-HCl (pH 7.5), 2.5 mM MgCl_2 , and 0.1 mM CaCl_2) or S1 nuclease buffer (30 mM sodium acetate (pH 4.5), 50 mM NaCl, and 1 mM ZnCl_2) with 0.05 $\mu\text{g}/\mu\text{l}$ calf thymus DNA (Sigma). The cleavage specificities of the enzymes used for DNA structure probing are as follows: DNase I, nonspecific cleavage and double-stranded DNA cleavage faster than cleavage of single-stranded DNA; MNase, single-stranded nucleic acid cleavage faster than cleavage of double-stranded nucleic acid (73); and S1 nuclease, specific for single-stranded nucleic acid. To avoid completely nonspecific cleavage, all digests were performed with limiting enzyme concentrations. DNase I digests were carried out in DNase I buffer using DNase I concentrations of 0.0125, 0.01, 0.0075, and 0.0005 units/ μl ; MNase digests were carried out in DNase I buffer using MNase concentrations of 0.0005, 0.00025, 0.0001, and 0.00005 units/ μl ; and S1 digests were performed in S1 nuclease buffer using S1 nuclease concentrations of 1, 0.5, and 0.1 unit/ μl . Reactions (final volume of 20 μl) were initiated by addition of 2 μl of the indicated nuclease and were incubated at 37 °C for 5 min. Reactions were terminated by 1:1 (v/v) phenol/chloroform extraction, followed by ethanol precipitation. The final DNA pellet was resuspended in 5 μl of formamide loading buffer; the products were separated by denaturing PAGE on a 6% gel.

Enzymatic Mapping of Acceptor RNAs—5′- ^{32}P -Labeled acceptor RNAs were gel-purified prior to use. Labeled RNA (~10 nM) was added to buffer containing 10 mM Tris-HCl (pH 7.0), 100 mM KCl, 10 mM MgCl_2 , and 1 μg of tRNA in a final volume of 10 μl . Reactions were initiated by addition of RNase V1, RNase T1, RNase A, or S1 nuclease and were incubated at room temperature for 15 min. Reactions were terminated by addition of precipitation buffer (Ambion Inc.). RNA pellets were resuspended in 5 μl of formamide loading buffer, and the products were resolved by denaturing PAGE on 6% gels. An alkaline hydrolysate was prepared by combining 0.15 pmol of ^{32}P -labeled RNA with 1 μg of tRNA in 50 mM sodium carbonate (pH 9.2) and 1 mM EDTA and then heating at 95 °C for 7 min. An additional RNase T1 digest was prepared by combining ^{32}P -labeled RNA in 20 mM sodium citrate (pH 7.5), 1 mM EDTA, and 7 M urea; heating at 65 °C for 5 min; adding RNase T1; and incubating for 15 min at room temperature. The reaction was terminated by addition of precipitation buffer, and the pelleted RNA was resuspended in 5 μl of formamide loading buffer prior to denaturing PAGE on a 6% gel.

RESULTS

Effect of 5′-Truncations of (–) SSDNA on Self-priming—The reconstituted minus-strand transfer system used in these

FIG. 1. Events occurring after the synthesis of HIV-1 (-) SSDNA, proposed secondary structure of TAR DNA, and (-) SSDNA constructs used in this study. A, schematic diagram illustrating two alternative pathways for RT-catalyzed elongation of (-) SSDNA. In the absence of acceptor RNA and NC, (-) SSDNA can form fold-back structures that undergo self-priming and subsequent formation of nonproductive SP DNAs. In this case, SP DNAs are the only products of reverse transcription. In the presence of acceptor RNA and NC, self-priming is inhibited, thereby allowing annealing of the complementary R regions within (-) SSDNA (see C) and acceptor RNA. Under these conditions, most of the products result from productive minus-strand transfer. Note that in the standard assay, (-) SSDNA and acceptor RNA are 128 and 148 nt in length, respectively. B, proposed secondary structure of TAR DNA. The proposed DNA structure is based on the complementary TAR RNA secondary structure (90, 91). For a lower energy TAR DNA structure based on mapping studies and *mFold* analysis (74), see Fig. 4B. C, series of synthetic HIV-1 (-) SSDNAs with truncations at the 5'-end used to test the effect of DNA length and structure on self-priming and minus-strand transfer. The R region is composed of TAR (open boxes) and additional 5'-upstream sequences (hatched boxes); U5 is represented as a closed box.



studies is illustrated in the schematic diagram in Fig. 1A. Strand transfer occurs in the presence of acceptor RNA and NC and is followed by RT-catalyzed elongation of (-) SSDNA (Fig. 1A). In the absence of NC, the TAR DNA structure in HIV-1 (-) SSDNA (Fig. 1B) induces nonproductive self-priming (Fig. 1A), which dramatically reduces the efficiency of minus-strand transfer (21, 23, 25, 51, 53, 55–57). Since disruption of the TAR DNA stem-loop by NC is required to block self-priming (25, 51, 56), it was of interest to examine the ability of NC to resolve highly structured regions within (-) SSDNA and the consequences for minus-strand transfer. To approach this question, we prepared a series of 5'-truncation mutants of full-length (-) SSDNA, which in our system is 128 nt (Fig. 1C). The 128-, 89-, 72-, 65-, 63-, and 59-nt synthetic (-) SSDNAs all contain sequences corresponding to the entire TAR DNA, whereas the remaining truncated DNAs have varying degrees of deletions within the TAR DNA sequence (Fig. 1C).

The amount of self-priming for each of the truncated (-) SSDNAs was determined by assay of DNA synthesis in the absence of acceptor RNA with or without NC; DNA products were visualized by PAGE (Fig. 2A). Self-priming occurs only if (-) SSDNA has a 5'-overhang as well as a base-paired 3'-end. Thus, (-) SSDNAs containing the full TAR DNA sequence and at least some short amount of additional 5'-R sequence, *i.e.* DNAs with lengths of 128, 89, 72, 69, 65, and 63 nt, readily

underwent self-priming (note black bars indicating SP products in each case). In contrast, with smaller (-) SSDNAs (Fig. 1C), *i.e.* having only the TAR sequence (59-nt DNA) or a truncation within TAR (50-nt DNA), self-priming could not be detected. Very similar results were obtained if self-priming was measured in reactions containing NC, but no acceptor, as also demonstrated in earlier studies (25, 56, 59).

The amount of SP DNAs synthesized by each of the (-) SSDNAs was quantified by PhosphorImager analysis of the gel data (Fig. 2B). For each of the DNAs, no significant difference was detected if NC was present in the reactions. Interestingly, the level of self-priming rose steeply as the 5'-DNA truncations extended into the R region upstream of TAR (compare the levels of self-priming observed for the 128-nt *versus* 89-nt (-) SSDNAs). However, when the truncations were extended within the TAR DNA stem-loop, self-priming was negligible (Fig. 2B) (data not shown). These findings suggest that disruption of the lower portion of the TAR DNA stem-loop (bases 3'-CCCCA paired to 5'-GGGT) (Fig. 1B) is sufficient to prevent self-priming.

Elimination of Self-priming Does Not Necessarily Increase the Efficiency of Minus-Strand Transfer—On the basis of our previous observations with 131-nt (21, 23, 51) and 128-nt (25) (-) SSDNAs, we would expect that an increase in self-priming should result in a decrease in minus-strand transfer, whereas

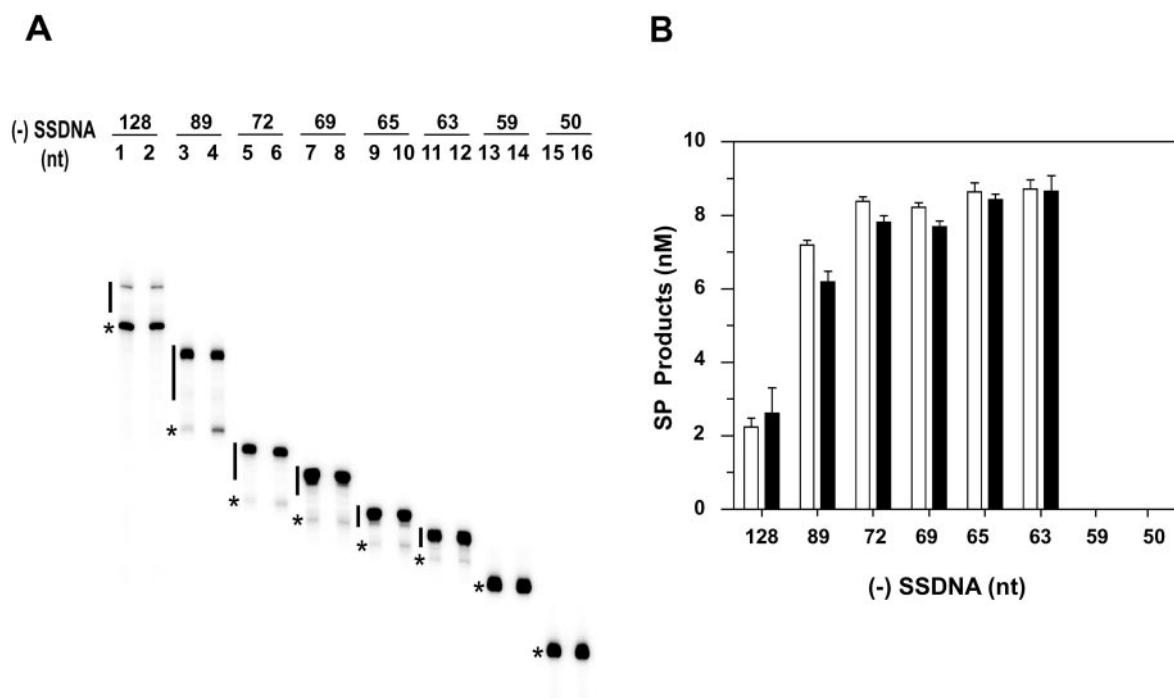


FIG. 2. **Effect of (-) SSDNA length on self-priming.** *A*, denaturing polyacrylamide gel showing self-priming of truncated (-) SSDNAs in the absence of acceptor with (even-numbered lanes) and without (odd-numbered lanes) NC. The reaction conditions are described under “Experimental Procedures,” except that incubation was for 60 min. Unextended (-) SSDNA, labeled at its 5'-end with ^{32}P , is indicated by asterisks; SP products are indicated by black bars. Note that data are also given for a 69-nt (-) SSDNA that has 4 additional 5'-terminal bases compared with the 65-nt (-) SSDNA (Fig. 1C). *B*, bar graph showing the amount of RT-catalyzed synthesis of SP products versus length of (-) SSDNA. Data represent the average values obtained for SP products in three independent experiments. Open bars, without NC; closed bars, with NC.

reduction or elimination of self-priming should increase strand transfer. To determine whether this prediction was also true when smaller (-) SSDNAs were used, we assayed strand transfer with each of the truncated DNAs under three conditions (Fig. 3A): without acceptor and NC (lanes 1, 4, and 7), with acceptor and without NC (lanes 2, 5, and 8), and with NC and acceptor (lanes 3, 6, and 9). The results of a typical gel analysis for reactions with 128-, 63-, and 50-nt (-) SSDNAs are shown. If NC and acceptor were omitted, the highest level of self-priming was observed with the 63-mer (lane 4); however, with the 50-mer, self-priming could not be detected (lane 7). In the absence of NC, addition of the 148-nt acceptor RNA, containing a 94-nt R region and 54 nt of U3 (51), resulted in low levels of strand transfer with each of the (-) SSDNAs (lanes 2, 5, and 8). Addition of NC and acceptor RNA dramatically increased the efficiency of minus-strand transfer with the 128-mer (lane 3), but, in the case of the 63-mer, did not significantly reduce the high level of self-priming and, at best, led to only minor stimulation of strand transfer (lane 6). Surprisingly, strand transfer was also inefficient with the 50-mer (lane 9), despite the absence of detectable self-priming. In fact, most of the input 50-mer remained after incubation under all three conditions (lanes 7–9).

The amount of transfer product synthesized in the presence of NC and acceptor RNA was quantified by PhosphorImager analysis and plotted against the length of (-) SSDNA (Fig. 3B). For the larger DNAs (63, 65, and 72 nt), high levels of self-priming were associated with reduced strand transfer, but low levels of self-priming observed with the smaller DNAs (59 nt and less) were not necessarily correlated with an increase in strand transfer (compare Figs. 2B and 3B). The highest level of strand transfer was obtained with the 128-mer, which contains all of the R region as well as 31 nt from the 5'-end of U5 (Fig. 1C). Strand transfer efficiency was reduced as truncations were made in the R region (89- and 72-mers) and was negligible

when the DNA truncations removed all or most of the R sequence upstream of TAR (65-, 63-, and 59-mers) or extended into TAR DNA itself (50-, 47-, and 30-mers). Quantitation of transfer products from several experiments performed in the presence of added NC and the 148-nt acceptor RNA is given in Table I (first line, second through fourth columns) for the 128-, 63-, and 50-nt (-) SSDNAs, respectively.

Secondary Structures of (-) SSDNAs and Efficiency of Minus-Strand Transfer—To understand why NC decreases self-priming and increases minus-strand transfer with some (-) SSDNAs but not with others, it was of interest to investigate the secondary structure of several of our (-) SSDNA constructs. For this purpose, each of the DNAs was subjected to limited nuclease digestion with DNase I, MNase, or S1 nuclease (Fig. 4A) (see “Experimental Procedures” for the cleavage specificity of each enzyme). We reasoned that comparison of the digest patterns generated with each of these nucleases should make it possible to obtain a general estimate of the relative double- versus single-stranded character of the DNAs.

Fig. 4A presents the nuclease digests; Fig. 4B shows the lowest energy structures predicted by DNA *m*Fold (74) that are most consistent with the nuclease digestion. The 128-, 63-, and 50-mer (-) SSDNAs were chosen for this analysis because they represent three different classes of activity in the minus-strand transfer assay with the 148-nt acceptor (Fig. 3): (i) DNA undergoes self-priming, which is decreased by NC (128-mer); (ii) DNA exhibits a high level of self-priming, which is relatively unaffected by NC (63-mer); and (iii) DNA exhibits little or no self-priming, but NC does not increase the level of minus-strand transfer (50-mer).

The nuclease digest pattern obtained with the 128-nt (-) SSDNA (Fig. 4A) indicated that it is single-stranded at its 5'-end; these bases are followed by a highly base-paired region immediately preceding nucleotides that comprise the TAR DNA stem-loop (nt 70–128). Nucleotides in the TAR DNA

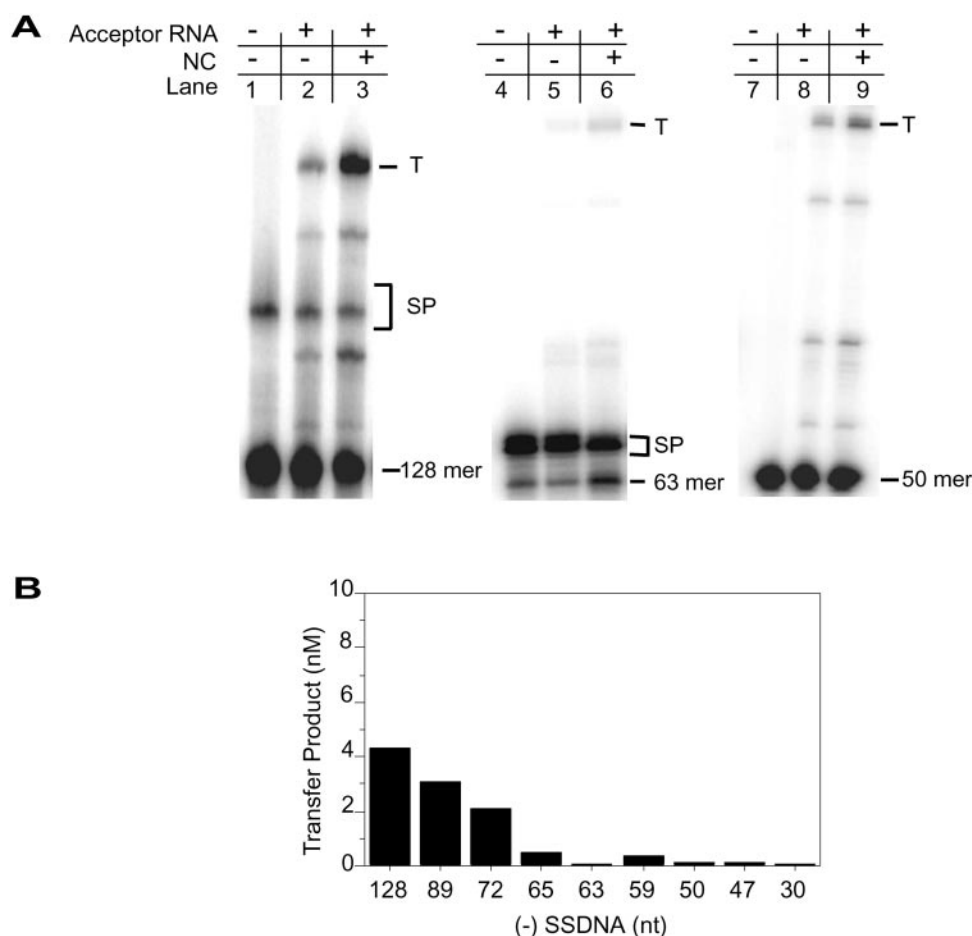


FIG. 3. Relationship between elimination of self-priming and the amount of productive minus-strand transfer. *A*, denaturing polyacrylamide gels indicating transfer products (*T*) and SP products formed with 128-, 63-, and 50-nt ^{32}P -labeled (-) SSDNAs (lanes 1–3, 4–6, and 7–9, respectively). Synthetic (-) SSDNAs were incubated at 37 °C for 30 min in the presence or absence of a 148-nt acceptor RNA with or without addition of HIV-1 NC as described under “Experimental Procedures.” *B*, bar graph showing the amount of minus-strand transfer product synthesized in the presence of NC as a function of the length of (-) SSDNA. The amount of transfer product was quantified as described under “Experimental Procedures.”

TABLE I

Effect of acceptor RNA length on NC-mediated minus-strand transfer with three representative (-) SSDNAs

Values were determined from the average of three to five individual experiments conducted in the presence of HIV-1 NC (nucleotide/NC ratio = 0.9:1).

RNA length	Transfer products		
	128-mer	63-mer	50-mer
<i>nt</i>	<i>nM</i>	<i>nM</i>	<i>nM</i>
148	3.8 ± 0.39	0.36 ± 0.20	0.12 ± 0.07
117	0.65 ± 0.37	0.38 ± 0.26	0.46 ± 0.26
100	0.40 ± 0.27	0.23 ± 0.093	0.26 ± 0.11
104	1.4 ± 0.55	1.8 ± 0.37	2.33 ± 1.7
87	1.4 ± 0.40	0.78 ± 0.69	1.9 ± 0.75
70	3.0 ± 0.48	4.5 ± 1.0	6.6 ± 0.89
84	1.4 ± 0.51	2.0 ± 0.28	2.1 ± 0.72
67	1.8 ± 0.45	2.4 ± 0.92	2.3 ± 0.69
50	0.76 ± 0.35	0.82 ± 0.086	1.4 ± 0.43

region of the 128-mer are also largely base-paired. Analysis of the 128-mer (-) SSDNA by *mFold* did not conclusively support a single unique structure. In fact, several structures of similar free energy were obtained (Fig. 4*B*, compare *inset* structure with lowest energy structure). These structures all have an unpaired 5'-end, followed by an extended stem-loop structure analogous to the predicted poly(A) hairpin (75, 76) near the 5'-end of HIV-1 genomic RNA. Surprisingly, none of the 128-mer structures contains a base-paired stem at the 3'-end that

would be compatible with the self-priming observed with this DNA (Figs. 2 and 3*A*). The low energetic threshold for conversion of these structures suggests that several structures may exist in solution, which may readily interconvert. Thus, it is possible that transient structures may exist, which can give rise to the observed SP products (for further discussion, see below).

The 63-mer, which consists of TAR DNA and just a few 5'-R sequences, was found to have a digest pattern consistent with the DNA being a mostly base-paired stem-loop structure (Fig. 4*A*). The lowest energy structure generated by *mFold* contains the TAR DNA stem-loop, including a large 13-nt internal loop with 7 nt on the 3'-side and 6 nt on the 5'-side (Fig. 4*B*), which is not present in higher energy TAR DNA structures (compare Figs. 1*B* and 4*B*). The structure shown in Fig. 4*B* is in general (although not complete) agreement with the observed digest pattern (Fig. 4, compare *A* and *B*). For example, the mapping data indicated that nt 1–11 are unpaired (Fig. 4*A*), yet *mFold* analysis predicted that nt 5–8 are base-paired (Fig. 4*B*). In the case of nt 50–55, which appeared to be in a double-stranded region, only nt 50–52 are expected to be base-paired. However, in the higher energy structure (Fig. 1*B*), nt 54 and 55 are also shown as base-paired. These differences between the mapping data and *mFold* predictions could be due to the fact that DNase I and MNase are not completely specific for digestion of double- and single-stranded DNAs, respectively. In addition, the mapping data might also reflect conformational heterogeneity of

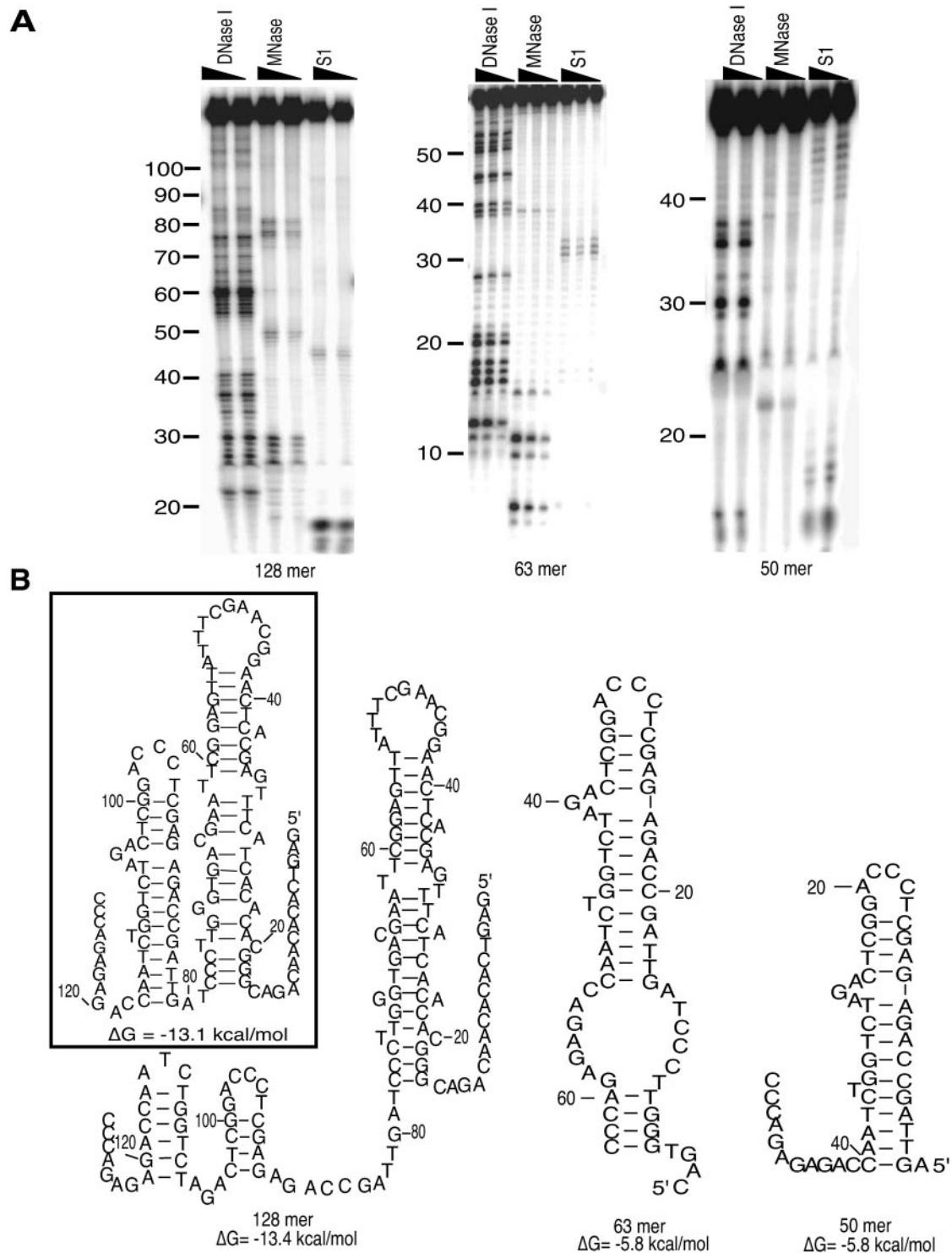


FIG. 4. Analysis of (-) SSDNA secondary structure. A, enzymatic mapping of ^{32}P -labeled (-) SSDNAs with lengths of 128, 63, and 50 nt. To estimate the relative double- versus single-stranded character of the (-) SSDNAs, each sample was subjected to limited digestion with DNase I, MNase, or S1 nuclease. It is important to note that the cleavage specificities for DNase I (double-stranded DNA cleavage faster than single-stranded DNA cleavage) and MNase (single-stranded nucleic acid cleavage faster than double-stranded nucleic acid cleavage) are not absolute (see “Enzymatic Mapping of (-) SSDNAs” under “Experimental Procedures”). The 128- and 50-nt (-) SSDNAs were digested with DNase I (0.0125 and 0.01 unit/ μl), MNase (0.0005 and 0.00025 units/ μl), or S1 nuclease (0.5 and 0.1 unit/ μl), and the 63-mer (-) SSDNA was digested with DNase I (0.01, 0.0075, and 0.005 units/ μl), MNase (0.00025, 0.0001, and 0.00005 units/ μl), or S1 nuclease (1, 0.5, and 0.1 unit/ μl) as described under “Experimental Procedures.” Numbering of nucleotides is from the 5'-end of each DNA (to the left of the gels). It should also be noted that when the enzymatic digestions were performed in reactions with NC, it was not possible to detect distinct gel bands, probably due to increased conformational heterogeneity of TAR DNA in the presence of NC (25, 60–62). B, secondary structure representations of the 128-, 63-, and 50-nt (-) SSDNAs based on *mFold* analysis (*mFold* Version 3.1) (74). Structures for the 63- and 50-mer (-) SSDNAs represent the lowest free energy structures that are most consistent with data obtained from enzymatic mapping (A) and the strand transfer assay (Fig. 3). The structure presented for the 128-nt (-) SSDNA represents the lowest free energy structure obtained. The *inset* 128-nt (-) SSDNA represents an alternative secondary structure that is nearly as favorable as the lowest energy structure. Structures were obtained by setting conditions to 37 °C with 75 mM monovalent ion and 7 mM MgCl_2 . The ΔG values in kilocalories/mol are shown in each case.

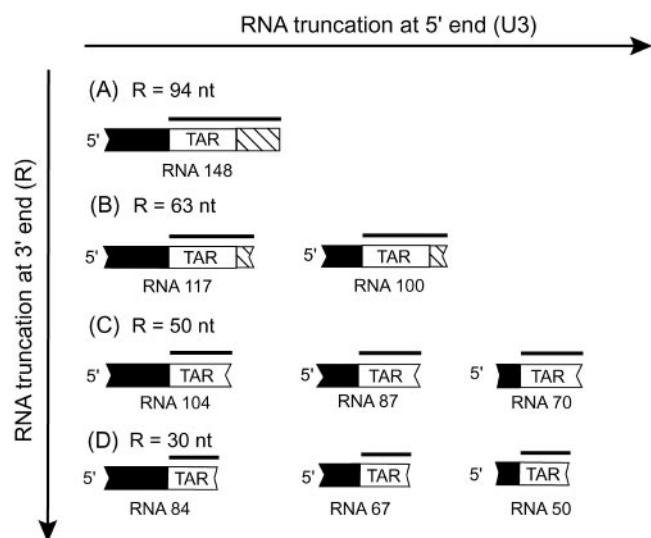


FIG. 5. Truncated acceptor RNAs used in this study. Four classes of RNA constructs were tested for their ability to facilitate efficient minus-strand transfer. The constructs varied in the length of U3 (5'-end; horizontal arrow) and the HIV-1 R region (3'-end; vertical arrow) contained within each construct: R regions of 94 nt (A), 63 nt (B), 50 nt (C), and 30 nt (D). For each of the constructs, the R region is indicated by a black bar over the 3'-end of the RNA. Additionally, within each class of RNA constructs, the length of the R region was maintained, whereas the 5'-end of the RNA was shortened. Regions at the 5'-end are indicated by closed boxes. TAR (open boxes) and upstream R sequences (hatched boxes) are indicated.

the TAR DNA structure in solution (25, 60–62), in particular transition between single-stranded and base-paired conformations at the base of the hairpin, as suggested for the 128-nt (–) SSDNA (see above). It is of interest that the loop residues (nt 30–33) present in all TAR DNA structures (compare Figs. 1B and 4B) were digested by the single strand-specific S1 nuclease (Fig. 4A). Moreover, the 4 free nucleotides at the 5'-end of the 63-mer (Fig. 4B) are consistent with the length of the SP product formed by this DNA (Figs. 2A and 3A).

In the case of the 50-mer (–) SSDNA, nt 17–20 as well as bases nearest the 3'-end (nt 40–50) were digested by S1 nuclease, indicating that these nucleotides are unpaired (Fig. 4A). The remaining nucleotides of this DNA were not significantly digested by either MNase or S1 nuclease, suggesting that these nucleotides are base-paired. The lowest energy structure predicted by *mFold* for the 50-mer DNA is in general agreement with the mapping data (Fig. 4, compare A and B). In addition, the observation that the 3'-end of the 50-mer DNA is largely unstructured and the 5'-end contains only 1 unpaired base would readily explain why this DNA does not undergo self-priming (Figs. 2 and 3A).

Truncation of Acceptor RNA Greatly Improves the Efficiency of Minus-Strand Transfer—Although the secondary structures observed for each of the (–) SSDNAs allow us to rationalize whether self-priming may or may not occur, these structures do not provide a complete explanation as to why there is such a striking reduction in the efficiency of strand transfer when (–) SSDNA is truncated (Fig. 3B), and the stabilities of these smaller DNAs are expected to favor formation of a DNA-RNA hybrid (Fig. 4B). These considerations suggested that in such cases, the acceptor RNA may not be able to anneal to the (–) SSDNA. This would occur if the acceptor RNA adopts a highly stable secondary structure.

To investigate this possibility, we prepared a series of RNA truncation mutants (Fig. 5). These RNAs were constructed to examine the effects of shortening the R region (3'-end), U3 (5'-end), or the R region and U3 on minus-strand transfer and

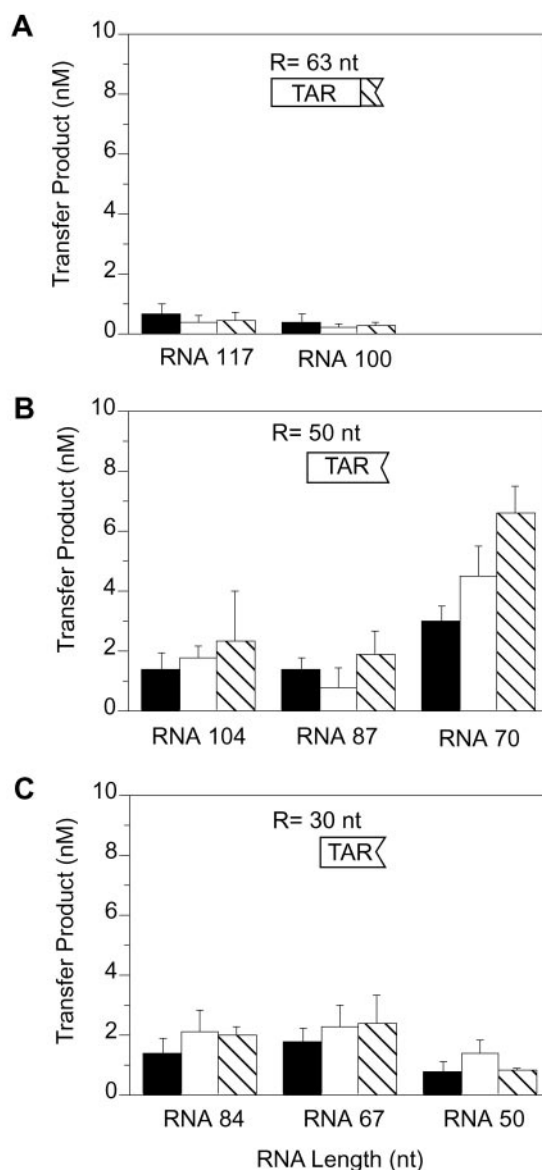


FIG. 6. Effect of acceptor RNA length on NC-mediated minus-strand transfer. Shown are the amounts of minus-strand transfer products obtained when the HIV-1 R region in the acceptor RNA was shortened to 63 nt (A), 50 nt (B), or 30 nt (C). A schematic version of the R region in each acceptor RNA is shown at the top of each panel; TAR (open boxes) and upstream R sequences (hatched box) are indicated. Each of the RNAs was tested with the following (–) SSDNAs: 128-mer (closed bars), 63-mer (open bars), and 50-mer (hatched bars). The effect of shortening the R region (3'-end of acceptor RNA) is shown by comparing the level of strand transfer in A–C, whereas the effect of shortening U3 (5'-end of acceptor RNA) is illustrated by comparing the level of strand transfer within each individual panel. Assays were conducted in the presence of HIV-1 NC at a ratio of one NC molecule to 0.9 nt. Data are average values obtained for strand transfer products in three to five individual experiments.

RNA structure. In the experiment illustrated in Fig. 6, we assayed the activities of three classes of acceptor RNAs, which we defined by the size of the R region (63, 50, and 30 nt); the size of the R region and a schematic diagram are shown at the top of each panel. Within each class, we have included two (Fig. 6A) or three (Fig. 6B and C) RNAs that have varying amounts of U3. All of the RNAs were assayed with the 128-, 63-, or 50-nt (–) SSDNAs in the presence of NC. The results are summarized in Table I.

One class of acceptor RNAs (RNAs 117 and 100) has the R region shortened from the wild-type 97 nt (70) to 63 nt, leaving

3'-sequences that correspond almost entirely to the TAR RNA stem-loop (Fig. 5B). The level of minus-strand transfer obtained with this acceptor RNA class and each of the (-) SSDNAs was quite low (Fig. 6A). For example, with the 128-mer (-) SSDNA, strand transfer was decreased by 5–6-fold compared with that observed with RNA 148 (R region equal to 94 nt) (Table I, second column, compare first line with second and third lines). When the R region was further truncated to 50 nt (Fig. 5C), there was a marked increase in strand transfer relative to the level observed with RNAs having an R region equal to 63 nt (Fig. 6, compare B with A). A modest increase in strand transfer was also seen with an RNA class that contained only 30 nt of the R sequence (Fig. 5D; and Fig. 6, compare C with A). These data show that the length of the R homology region is not the sole indicator for predicting successful strand transfer. Importantly, the results also demonstrate that the full-length R region is not required for efficient minus-strand transfer.

To determine whether the size of U3 and that of the R region influence minus-strand transfer, we examined the effect of shortening U3 in the acceptor RNAs of each class. In the class with an R region equal to 63 nt (Figs. 5B and 6A), two RNAs were tested: RNA 117, containing 54 nt of U3 (the same as RNA 148 (Fig. 5A)), and RNA 100, containing 38 nt of U3. With RNA 117, strand transfer was poor regardless of which (-) SSDNA was used (Fig. 6A and Table I, second line). Further truncation of U3 to 38 nt to disrupt additional RNA secondary structure did not increase the level of minus-strand transfer with any of the (-) SSDNAs tested (Fig. 6A and Table I, third line) (data not shown). In contrast, when the R region was maintained at 50 nt (Figs. 5C and 6B), truncation of U3 resulted in a significant stimulation of minus-strand transfer. In particular, shortening U3 to 20 nt (RNA 70) led to a >50-fold increase in the level of minus-strand transfer with the 50-nt (-) SSDNA compared with transfer with this DNA and RNA 148 (compare Figs. 3 and 6B; and Table I, last column, compare first and sixth lines). In addition, we observed that self-priming from the 63-nt (-) SSDNA was diminished when RNA 70 was used as the acceptor (data not shown). Taken together, the results in Fig. 6 (A and B) indicate that stable structure in the acceptor RNA lowers the efficiency of strand transfer.

Interestingly, if the R region was maintained at 30 nt, additional 5'-truncations in U3 (RNAs 67 and 50) (Fig. 5D) led to a tapering off of the level of minus-strand transfer (Fig. 6C). This was most striking when the activities of RNA 70 (Fig. 6B and Table I, sixth line) and RNA 50 (Fig. 6C and Table I, ninth line) were compared. Thus, simply truncating the acceptor RNA does not always result in enhanced strand transfer efficiency (see below).

RNA Structure Is Important for Predicting the Efficiency of NC-mediated Minus-Strand Transfer—To confirm that a high degree of structure in the acceptor RNAs interferes with the efficiency of NC-mediated minus-strand transfer, we subjected several of our truncation mutants to limited RNase digestion and analysis by *mFold* (Fig. 7) (75, 76). Fig. 7A presents the RNase digest patterns generated for RNAs containing the following lengths of the R region: 94 nt (RNA 148), 63 nt (RNA 117), and 50 nt (RNAs 104 and 70). The two RNAs with an R region equal to 50 nt were chosen to examine whether significant changes in structure occur with additional truncation of U3. The cleavage specificity for each of the enzymes is given in the legend to Fig. 7A.

For RNAs 148, 117, and 104, regions within TAR expected to be largely single-stranded (nt 77–79 and 84–89) were digested by RNase T1 (3 G residues, nt 86–88) (Fig. 7A, lanes 7), RNase A (UCU (nt 77–79) and C (nt 84)) (lanes 3 and 4), and S1 nuclease (U (nt 85)) (lanes 5 and 6). Despite truncation into the

TAR stem, nt 55–63 in RNA 104 as well as in RNAs 128 and 117 remained largely under-digested by RNases T1 and A, suggesting that the lower portion of the TAR stem-loop structure maintains a mostly base-paired conformation. In addition, other nucleotides in RNAs 148, 117, and 104, including those in the 3'-half of the TAR stem-loop (nt 90–113 in RNAs 148 and 117 and nt 90–104 in RNA 104), underwent a varying amount of digestion by nuclease V1 (lanes 1 and 2). Taken together, the data are consistent with the structure being predominantly helical in nature. Interestingly, the digest patterns at the 5'-ends of these RNAs were very similar: digestion of nt 50–53 by RNase A (lanes 3 and 4), S1 nuclease (lanes 5 and 6), and RNase T1 (lanes 7); digestion by RNase A (lanes 3 and 4) and S1 nuclease (lanes 5 and 6) in the region of nt 40–49; and strong digestion by RNase A (lanes 3 and 4) and S1 nuclease (lanes 5 and 6) around nt 30. The similarity of the digest patterns observed for each of the three RNAs suggests a high degree of secondary structure conservation, even when the R region was significantly truncated (Fig. 5).

Indeed, when *mFold* analysis (75, 76) was performed on these RNAs using some double- and single-strand constraints based on the results of the RNase digestions, very similar structures were obtained (Fig. 7B). Most notably, we found that even though sequences of the TAR RNA stem-loop were removed in RNA 104, the lower portion of the stem-loop could be reconstituted with sequences from the 5'-end of the RNA. Moreover, the free energy values obtained for each of the RNAs demonstrated that these RNAs fold into very stable secondary structures. These results are consistent with the strand transfer data showing that with one exception (148-nt acceptor and 128-nt (-) SSDNA; see below), RNAs 148 and 117 supported low levels of strand transfer; in contrast, RNA 104, which has a high ΔG value (but significantly lower than the ΔG values of the two larger RNAs) (Fig. 7B), exhibited moderate strand transfer activity with the 128-, 63-, and 50-nt (-) SSDNAs (Fig. 6, A and B, and Table I, first, second, and fourth lines).

Similarly, RNA 70 exhibited many of the characteristic RNase digestion properties expected for the TAR RNA stem-loop. In particular, the TAR loop (nt 50–55) was maintained: nt 52–54 were digested by S1 nuclease (Fig. 7A, lanes 5 and 6) and RNase T1 (lane 7). The C residue at nt 50 and the bulge region (nt 43–45) were digested by RNase A (lanes 3 and 4). However, the overall decrease in the length of RNA 70 led to disruption of the remainder of the lower half of the TAR stem, and two shorter stem-loop structures at the 5'-end were formed instead (Fig. 7B). In particular, nt 24–26 and 34, which correspond to nt 58–60 and 68, respectively, in the larger RNAs and are normally paired in the TAR stem-loop, were digested by RNase A (Fig. 7, A, lanes 3 and 4; and B). Thus, disruption of the TAR stem leads to an overall reduction in the stability of RNA 70, which facilitates NC-mediated annealing of (-) SSDNA to acceptor RNA and subsequent strand transfer (Fig. 6B and Table I, sixth line).

Decreasing the Stability of Both (-) SSDNA and Acceptor RNA Eliminates the Requirement for NC—The results presented thus far indicate that (-) SSDNA and acceptor RNA structure and stability have a significant effect on the ability of NC to facilitate minus-strand transfer. Thus, NC was unable to stimulate strand transfer in reactions containing a stable RNA and a (-) SSDNA that is capable of a high degree of self-priming (Fig. 3A, compare lanes 5 and 6). These findings led us to predict that for reactions with a (-) SSDNA that does not self-prime and an acceptor RNA containing little secondary structure, addition of NC should have little or no effect on minus-strand transfer efficiency.

To test this hypothesis, we assayed minus-strand transfer

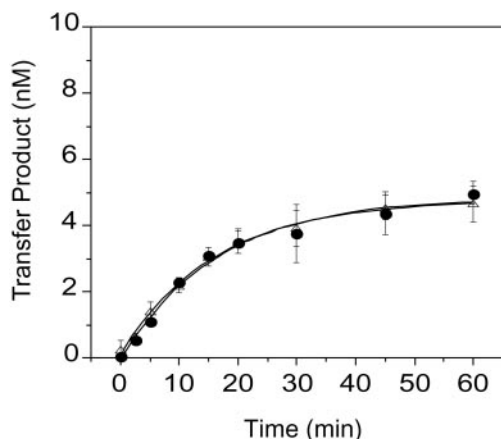


FIG. 8. Kinetics of minus-strand transfer with the 50-nt (-) SSDNA and 70-nt acceptor RNA in the presence or absence of NC. The amount of minus-strand transfer product synthesized is plotted as a function of time. Standard reaction mixtures with and without NC and containing the 50-nt (-) SSDNA and 70-nt acceptor RNA were scaled up to a final volume of 100 μ l, and 10- μ l aliquots were removed at the indicated times. Data were fit to a single exponential equation and gave the following k_{obs} values: with NC (Δ), $k_{\text{obs}} = 0.062 \pm 0.0047 \text{ min}^{-1}$; and without NC (\bullet), $k_{\text{obs}} = 0.061 \pm 0.0077 \text{ min}^{-1}$.

synthesized in both reactions at the end point (60 min). These results clearly illustrate the delicate balance that exists between RNA and DNA stability and the ability of NC to mediate successful minus-strand transfer.

DISCUSSION

In this study, we have performed a systematic analysis to understand how the nucleic acid chaperone activity of NC is affected by varying degrees of stable secondary structure in either (-) SSDNA or acceptor RNA (or both) during minus-strand transfer. We found that alterations in the secondary structure of (-) SSDNA resulted in dramatic fluctuations in the level of nonproductive DNA self-priming. However, elimination of secondary structures responsible for self-priming did not necessarily increase strand transfer efficiency: secondary structure of the acceptor RNA was also critical. Indeed, little or no strand transfer was observed when the acceptor was highly structured, regardless of whether NC was present. Collectively, these results reinforce the idea that the nucleic acid chaperone activity of NC favors formation of the most thermodynamically stable structure, which in some circumstances will not be the strand transfer duplex.

The presence of the TAR DNA stem-loop at the 3'-end of (-) SSDNA has been shown to induce RT-catalyzed synthesis of the majority of SP products observed *in vitro* (25, 51, 53, 56, 58, 59). Since the TAR DNA structure is not necessarily present in the lowest energy structure of HIV-1 (-) SSDNA (59) and since a complex mixture of SP DNAs is observed during synthesis of (-) SSDNA (51), it is formally possible that other structures might also be involved. However, self-priming was highest when (-) SSDNA contained little more than the TAR DNA sequence (63-nt (-) SSDNA) (Fig. 2), and even small disruptions of the TAR DNA stem-loop resulted in elimination of SP products (50-nt (-) SSDNA) (Figs. 2 and 3A). This result is consistent with earlier work demonstrating that deletion of 19 nt at the 3'-end of the TAR DNA stem-loop eliminates self-priming (51). Mutations that convert bulges in the lower portion of TAR DNA to paired bases (56, 62) reduce the ability of NC to destabilize the structure (62) and lead to an increase in self-priming (56). Recent studies also show that NC destabilizes the bottom half of TAR DNA more efficiently than the upper half (62, 63). It is of interest that in the absence of acceptor, NC has little or no effect on the amount of SP prod-

ucts that are synthesized (Fig. 2) (25, 56, 59).

The level of self-priming is related to the stability of fold-back structures formed at the 3'-end of (-) SSDNA rather than to the complexity of the R region (59). For example, self-priming of the 128-nt (-) SSDNA ($\Delta G = -13.1$ or -13.4 kcal/mol) was 2–3-fold lower than that observed for other smaller TAR DNA-containing (-) SSDNAs with lower overall stabilities (Figs. 2 and 4B). Interestingly, *mFold* analysis of the 128-nt (-) SSDNA predicted that the lowest energy structures have unpaired bases at their 3'-ends and that in one of the predicted structures ($\Delta G = -13.4 \text{ kcal/mol}$), a recognizable TAR DNA stem-loop is not formed (Fig. 4B). Thus, self-priming may be lower for this DNA because the TAR DNA stem-loop structure with 3'-paired bases is not present in a significant portion of the population. (Of course, at least some of the DNA molecules must contain the TAR DNA stem-loop since SP products were observed experimentally (Figs. 2 and 3A).)

Analysis of the isolated TAR DNA structure by fluorescence spectroscopy provides strong evidence that the DNA population consists of a heterogeneous mixture of conformers (25, 60–62). Thus, we expect that increasing the length of (-) SSDNA results in an increase in the conformational complexity of the DNA population, leading to disruption of TAR DNA in favor of conformers with 3'-single-stranded extensions. These considerations could explain why SP products are not observed in endogenous reverse transcription assays (51). It is also possible that during endogenous reverse transcription or virus replication, some of the (-) SSDNA remains transiently bound to 5'-terminal fragments from the initial genomic RNA template, which (since NC is present) would prevent formation of fold-back structures and self-priming (56). However, this alone would not necessarily increase the efficiency of strand transfer.

Indeed, our data lead to the major conclusion that elimination of self-priming is not sufficient to promote an increase in the level of minus-strand transfer in the presence of NC and acceptor RNA (Fig. 3). This result was initially somewhat surprising and suggested that NC might not always be capable of mediating the formation of the DNA-RNA duplex. We considered the possibility that the degree of complementarity between the R regions in the acceptor RNA and the truncated (-) SSDNAs is important. In the case of the 128-nt (-) SSDNA, the highest level of strand transfer occurred in reactions containing the 148-nt acceptor RNA (Fig. 3 and Table I, second column). This finding could be explained, at least in part, by the fact that annealing of 94 nt in the R region leads to formation of a more stable duplex than is possible with smaller R regions.

However, the experiments described in Fig. 6 clearly show that the length of the R region in the acceptor RNA and (-) SSDNA is not always a primary determinant of efficient minus-strand transfer. For example, when the R region in the acceptor RNA was reduced from 63 to 50 nt, the level of strand transfer was increased with each of the (-) SSDNAs tested (Fig. 6, compare A and B). Thus, in our system, the extent of sequence complementarity between (-) SSDNA and the acceptor RNA need not be extremely long for successful minus-strand transfer. This result is in excellent agreement with previous studies showing that the full-length R region is not required for minus-strand transfer both *in vivo* and *in vitro* (26, 44, 51, 77–79). Similarly, the size of the homology region is not the most critical factor for efficient recombination via internal strand transfer (80).

Alternatively, the presence of highly stable structures in the acceptor RNA (Fig. 7B) that prevent annealing of (-) SSDNA to the acceptor RNA might account for the low level of strand transfer obtained with the small (-) SSDNAs and the 148-nt acceptor RNA (Fig. 3 and Table I, first line). Although anneal-

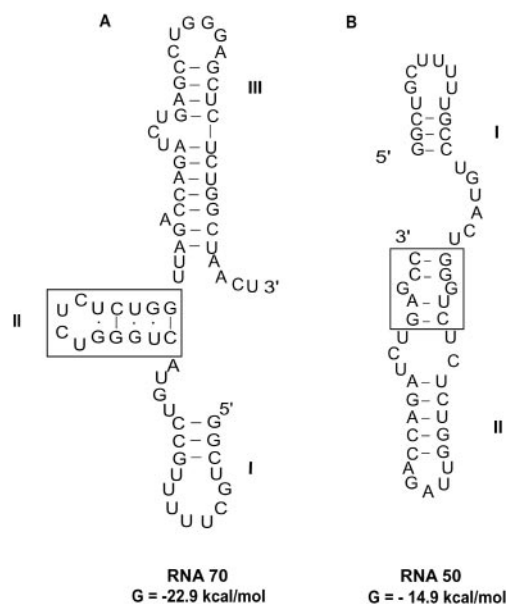


FIG. 9. Comparison of structures predicted by *mFold* for RNAs 70 and 50. The predicted structures and ΔG values for RNA 70 (A) and RNA 50 (B) are shown. The boxed nucleotides represent potential NC-binding sites.

ing was not measured directly in this study, it is expected that the conformational stability of the DNA and RNA strands will affect annealing and elongation of minus-strand DNA by RT, which in turn will impact overall strand transfer and the extent of self-priming. In fact, in previous reports, we showed that reduction of NC-mediated annealing could be correlated with a reduction in strand transfer (17, 23).

The importance of acceptor RNA structure in strand transfer is illustrated by the data in Fig. 6 and has also been reported in several other studies (66, 67, 80–84). Interestingly, an important conclusion of this work is that the highest levels of strand transfer occur when the structures in both (–) SSDNA and acceptor RNA are significantly disrupted (Figs. 4B, 6B, and 7B and Table I). This finding indicates that NC exerts its effect upon both DNA and RNA secondary structures. The fact that minus-strand transfer appears to be particularly sensitive to excessively stable structure in the acceptor RNA and to a somewhat smaller extent to the structure in (–) SSDNA is consistent with the fact that NC induces only very limited melting of the TAR RNA structure compared with melting of the TAR DNA stem-loop (60). It has also been reported that introduction of stabilizing mutations in the poly(A) stem-loop of the acceptor RNA inhibits productive minus-strand transfer (81).

Another important conclusion of this work is that the effect of NC is evident only in the case of structures that are partially but not completely destabilized. Using the truncated 50-nt (–) SSDNA and RNA 70 acceptor, whose stabilities were significantly decreased relative to larger constructs (Figs. 4B and 7B), we found that NC did not increase either the rate or extent of minus-strand transfer (Fig. 8). Similarly, NC has little effect on the rate of annealing of short DNA oligonucleotides when these oligonucleotides are unstructured, whereas NC increases the rate of annealing when secondary structure is present (26). Moreover, NC exerts little effect on weakly structured regions of the HIV-1 RNA genome during internal strand transfer (66) or on model RNAs with low ΔG values in an annealing reaction (67).

Thus far, we have discussed NC nucleic acid chaperone activity in terms of the overall thermodynamic stability of the nucleic acid reactants in minus-strand transfer. We note one

exception, however, concerning the activities of RNAs 70 and 50 in minus-strand transfer assays with the 128-, 63-, and 50-nt (–) SSDNAs (Fig. 6, compare B with C). Paradoxically, strand transfer was considerably more efficient with RNA 70 than with RNA 50, even though on the basis of *mFold* analysis, RNA 70 ($\Delta G = -22.9 \text{ kcal/mol}$) (Figs. 7B and 9A) is more stable than RNA 50 ($\Delta G = -14.9 \text{ kcal/mol}$) (Fig. 9B). In this case, local structure at favorable NC-binding sites (e.g. a run of G or UG residues (22, 85–89)) appears to differ. In particular, UG-rich stem-loop II of RNA 70 (Fig. 9A, boxed nucleotides) contains bases (5'-GGGUC...) that are complementary to sequences in TAR at the 3'-end of the (–) SSDNA constructs and is a likely site for initiation of the annealing reaction. This stem-loop contains a relatively weak helix with three G-U wobble pairs and only two G-C base pairs. In contrast, the corresponding sequence in RNA 50 is part of stem-loop II and contains three stabilizing G-C base pairs as well as a single destabilizing G-G mismatch (Fig. 9B, boxed nucleotides). We speculate that RNA 70 has more activity in minus-strand transfer because the weak stem-loop II in RNA 70 is a more favorable site for initiating the annealing reaction than stem-loop II in RNA 50. Thus, we suggest that the effectiveness of NC nucleic acid chaperone activity is ultimately dependent on the stability of local structure rather than on the stability of the overall structure. This conclusion is in accord with the results of a recent kinetic and thermodynamic study of tRNA^{Lys} annealing to the 18-nt primer-binding site in an HIV-1 genomic RNA transcript (33). Experiments to further test our hypothesis in the minus-strand transfer system are now in progress.

In summary, our results demonstrate that the stability and structure of both (–) SSDNA and acceptor RNA play a role in the ability of NC to efficiently mediate minus-strand transfer. Enzymatic mapping studies, together with *mFold* analysis, demonstrated that the R region of the 148-nt acceptor RNA is highly structured and that significant truncation of this RNA is required to decrease its stability (Fig. 7) so that efficient strand transfer may occur. It has been proposed that NC decreases self-priming in (–) SSDNA by binding to the DNA as it undergoes normal conformational fluctuations, resulting in an increased proportion of the DNA population in various unfolded and semi-folded states (25, 60–62), with the greatest shift to less folded states occurring when acceptor RNA is present (25). Similarly, we envision that transient conformational fluctuations of the RNA will allow binding of NC and a subsequent redistribution in the number and types of conformations accessible to the RNA. A change in the equilibrium distribution of RNA conformations might be expected to require interaction with a (–) SSDNA. Thus, an important criterion for efficient strand transfer is the maintenance of a delicate thermodynamic balance between structures present in the RNA or DNA and the stability of the strand transfer duplex.

Acknowledgments—We are grateful to Dr. Robert Gorelick for the generous gift of recombinant HIV-1 NC. We also thank Drs. Karin Musier-Forsyth, Jianhui Guo, and Ioulia Rouzina for valuable discussion and critical reading of the manuscript; Drs. Jianhui Guo and Yasumasa Iwatani for gracious help with preparation of the figures for publication; and Klara Post for editorial assistance.

REFERENCES

- Coffin, J. M., Hughes, S. H., and Varmus, H. E. (1997) *Retroviruses*, Cold Spring Harbor Laboratory, Cold Spring Harbor, NY
- Henderson, L. E., Copeland, T. D., Sowder, R. C., Smythers, G. W., and Oroszlan, S. (1981) *J. Biol. Chem.* **256**, 8400–8406
- Green, L. M., and Berg, J. M. (1990) *Proc. Natl. Acad. Sci. U. S. A.* **87**, 6403–6407
- South, T. L., Blake, P. R., Sowder, R. C., III, Arthur, L. O., Henderson, L. E., and Summers, M. F. (1990) *Biochemistry* **29**, 7786–7789
- Summers, M. F., South, T. L., Kim, B., and Hare, D. R. (1990) *Biochemistry* **29**, 329–340
- Lorsch, J. R. (2002) *Cell* **109**, 797–800
- Tsuchihashi, Z., and Brown, P. O. (1994) *J. Virol.* **68**, 5863–5870

8. Darlix, J.-L., Lapadat-Tapolksy, M., de Rocquigny, H., and Roques, B. P. (1995) *J. Mol. Biol.* **254**, 523–537
9. Herschlag, D. (1995) *J. Biol. Chem.* **270**, 20871–20874
10. Rein, A., Henderson, L. E., and Levin, J. G. (1998) *Trends Biochem. Sci.* **23**, 297–301
11. Cristofari, G., and Darlix, J.-L. (2002) *Prog. Nucleic Acid Res. Mol. Biol.* **72**, 223–268
12. de Rocquigny, H., Gabus, C., Vincent, A., Fournié-Zaluski, M.-C., Roques, B., and Darlix, J.-L. (1992) *Proc. Natl. Acad. Sci. U. S. A.* **89**, 6472–6476
13. Dib-Hajj, F., Khan, R., and Giedroc, D. P. (1993) *Protein Sci.* **2**, 231–243
14. You, J. C., and McHenry, C. S. (1994) *J. Biol. Chem.* **269**, 31491–31495
15. Lapadat-Tapolksy, M., Pernelle, C., Borie, C., and Darlix, J.-L. (1995) *Nucleic Acids Res.* **23**, 2434–2441
16. Davis, W. R., Gabbara, S., Hupe, D., and Peliska, J. A. (1998) *Biochemistry* **37**, 14213–14221
17. Guo, J., Wu, T., Bess, J., Henderson, L. E., and Levin, J. G. (1998) *J. Virol.* **72**, 6716–6724
18. Auxilien, S., Keith, G., Le Grice, S. F. J., and Darlix, J.-L. (1999) *J. Biol. Chem.* **274**, 4412–4420
19. Chan, B., Weidemaier, K., Yip, W.-T., Barbara, P. F., and Musier-Forsyth, K. (1999) *Proc. Natl. Acad. Sci. U. S. A.* **96**, 459–464
20. Wu, T., Guo, J., Bess, J., Henderson, L. E., and Levin, J. G. (1999) *J. Virol.* **73**, 4794–4805
21. Guo, J., Wu, T., Anderson, J., Kane, B. F., Johnson, D. G., Gorelick, R. J., Henderson, L. E., and Levin, J. G. (2000) *J. Virol.* **74**, 8980–8988
22. Johnson, P. E., Turner, R. B., Wu, Z. R., Hairston, L., Guo, J., Levin, J. G., and Summers, M. F. (2000) *Biochemistry* **39**, 9084–9091
23. Guo, J., Wu, T., Kane, B. F., Johnson, D. G., Henderson, L. E., Gorelick, R. J., and Levin, J. G. (2002) *J. Virol.* **76**, 4370–4378
24. Urbaneja, M. A., Wu, M., Casas-Finet, J. R., and Karpel, R. L. (2002) *J. Mol. Biol.* **318**, 749–764
25. Hong, M. K., Harbron, E. J., O'Connor, D. B., Guo, J., Barbara, P. F., Levin, J. G., and Musier-Forsyth, K. (2003) *J. Mol. Biol.* **325**, 1–10
26. Golinelli, M.-P., and Hughes, S. H. (2003) *Biochemistry* **42**, 8153–8162
27. Ji, X., Klarmann, G. J., and Preston, B. D. (1996) *Biochemistry* **35**, 132–143
28. Wu, W., Henderson, L. E., Copeland, T. D., Gorelick, R. J., Bosche, W. J., Rein, A., and Levin, J. G. (1996) *J. Virol.* **70**, 7132–7142
29. Drummond, J. E., Mounts, P., Gorelick, R. J., Casas-Finet, J. R., Bosche, W. J., Henderson, L. E., Waters, D. J., and Arthur, L. O. (1997) *AIDS Res. Hum. Retroviruses* **13**, 533–543
30. Zhang, W. H., Hwang, C. K., Hu, W.-S., Gorelick, R. J., and Pathak, V. K. (2002) *J. Virol.* **76**, 7473–7484
31. Khan, R., and Giedroc, D. P. (1992) *J. Biol. Chem.* **267**, 6689–6695
32. Hargittai, M. R. S., Mangla, A. T., Gorelick, R. J., and Musier-Forsyth, K. (2001) *J. Mol. Biol.* **312**, 985–997
33. Hargittai, M. R. S., Gorelick, R. J., Rouzina, I., and Musier-Forsyth, K. (2004) *J. Mol. Biol.* **337**, 951–968
34. Tisné, C., Roques, B. P., and Dardel, F. (2003) *Biochimie (Paris)* **85**, 557–561
35. Prats, A. C., Sarih, L., Gabus, C., Litvak, S., Keith, G., and Darlix, J.-L. (1988) *EMBO J.* **7**, 1777–1783
36. Barat, C., Lullien, V., Schatz, O., Keith, G., Nugeyre, M. T., Grüniger-Leitch, F., Barré-Sinoussi, F., Le Grice, S. F. J., and Darlix, J.-L. (1989) *EMBO J.* **8**, 3279–3285
37. Cen, S., Huang, Y., Khorchid, A., Darlix, J.-L., Wainberg, M. A., and Kleiman, L. (1999) *J. Virol.* **73**, 4485–4488
38. Feng, Y.-X., Campbell, S., Harvin, D., Ehresmann, B., Ehresmann, C., and Rein, A. (1999) *J. Virol.* **73**, 4251–4256
39. Rong, L., Liang, C., Hsu, M., Kleiman, L., Petitjean, P., de Rocquigny, H., Roques, B. P., and Wainberg, M. A. (1998) *J. Virol.* **72**, 9353–9358
40. Rong, L., Liang, C., Hsu, M., Guo, X., Roques, B. P., and Wainberg, M. A. (2001) *J. Biol. Chem.* **276**, 47725–47732
41. Iwatani, Y., Rosen, A. E., Guo, J., Musier-Forsyth, K., and Levin, J. G. (2003) *J. Biol. Chem.* **278**, 14185–14195
42. Muthuswami, R., Chen, J., Burnett, B. P., Thimmig, R. L., Janjic, N., and McHenry, C. S. (2002) *J. Mol. Biol.* **315**, 311–323
43. Telesnitsky, A., and Goff, S. P. (1993) in *Reverse Transcriptase* (Skalka, A. M., and Goff, S. P., eds) pp. 49–83, Cold Spring Harbor Laboratory, Cold Spring Harbor, NY
44. Chen, Y., Balakrishnan, M., Roques, B. P., Fay, P. J., and Bambara, R. A. (2003) *J. Biol. Chem.* **278**, 8006–8017
45. Chen, Y., Balakrishnan, M., Roques, B. P., and Bambara, R. A. (2003) *J. Biol. Chem.* **278**, 38368–38375
46. Darlix, J.-L., Vincent, A., Gabus, C., de Rocquigny, H., and Roques, B. (1993) *C. R. Acad. Sci. (Paris) Life Sci.* **316**, 763–771
47. Allain, B., Lapadat-Tapolksy, M., Berlioz, C., and Darlix, J.-L. (1994) *EMBO J.* **13**, 973–981
48. Peliska, J. A., Balasubramanian, S., Giedroc, D. P., and Benkovic, S. J. (1994) *Biochemistry* **33**, 13817–13823
49. DeStefano, J. J. (1995) *Arch. Virol.* **140**, 1775–1789
50. Rodriguez-Rodriguez, L., Tsuchihashi, Z., Fuentes, G. M., Bambara, R. A., and Fay, P. J. (1995) *J. Biol. Chem.* **270**, 15005–15011
51. Guo, J., Henderson, L. E., Bess, J., Kane, B., and Levin, J. G. (1997) *J. Virol.* **71**, 5178–5188
52. Kim, J. K., Palaniappan, C., Wu, W., Fay, P. J., and Bambara, R. A. (1997) *J. Biol. Chem.* **272**, 16769–16777
53. Lapadat-Tapolksy, M., Gabus, C., Rau, M., and Darlix, J.-L. (1997) *J. Mol. Biol.* **268**, 250–260
54. Negroni, M., and Buc, H. (1999) *J. Mol. Biol.* **286**, 15–31
55. Brulé, F., Bec, G., Keith, G., Le Grice, S. F. J., Roques, B. P., Ehresmann, B., Ehresmann, C., and Marquet, R. (2000) *Nucleic Acids Res.* **28**, 634–640
56. Driscoll, M. D., and Hughes, S. H. (2000) *J. Virol.* **74**, 8785–8792
57. Li, X., Quan, Y., Arts, E. J., Li, Z., Preston, B. D., de Rocquigny, H., Roques, B. P., Darlix, J.-L., Kleiman, L., Parniak, M. A., and Wainberg, M. A. (1996) *J. Virol.* **70**, 4996–5004
58. Driscoll, M. D., Golinelli, M.-P., and Hughes, S. H. (2001) *J. Virol.* **75**, 672–686
59. Golinelli, M.-P., and Hughes, S. H. (2001) *Virology* **285**, 278–290
60. Bernacchi, S., Stoylov, S., Piémont, E., Ficheux, D., Roques, B. P., Darlix, J.-L., and Mély, Y. (2002) *J. Mol. Biol.* **317**, 385–399
61. Azoulay, J., Clamme, J.-P., Darlix, J.-L., Roques, B. P., and Mély, Y. (2003) *J. Mol. Biol.* **326**, 691–700
62. Beltz, H., Azoulay, J., Bernacchi, S., Clamme, J.-P., Ficheux, D., Roques, B., Darlix, J.-L., and Mély, Y. (2003) *J. Mol. Biol.* **328**, 95–108
63. Beltz, H., Piémont, E., Schaub, E., Ficheux, D., Roques, B., Darlix, J.-L., and Mély, Y. (2004) *J. Mol. Biol.* **338**, 711–723
64. Williams, M. C., Rouzina, I., Wenner, J. R., Gorelick, R. J., Musier-Forsyth, K., and Bloomfield, V. A. (2001) *Proc. Natl. Acad. Sci. U. S. A.* **98**, 6121–6126
65. Williams, M. C., Gorelick, R. J., and Musier-Forsyth, K. (2002) *Proc. Natl. Acad. Sci. U. S. A.* **99**, 8614–8619
66. Derebail, S. S., Heath, M. J., and DeStefano, J. J. (2003) *J. Biol. Chem.* **278**, 15702–15712
67. Heath, M. J., Derebail, S. S., Gorelick, R. J., and DeStefano, J. J. (2003) *J. Biol. Chem.* **278**, 30755–30763
68. Moscardini, M., Pistello, M., Bendinelli, M., Ficheux, D., Miller, J. T., Gabus, C., Le Grice, S. F. J., Surewicz, W. K., and Darlix, J.-L. (2002) *J. Mol. Biol.* **318**, 149–159
69. Lee, N., Gorelick, R. J., and Musier-Forsyth, K. (2003) *Nucleic Acids Res.* **31**, 4847–4855
70. Adachi, A., Gendelman, H. E., Koenig, S., Folks, T., Willey, R., Rabson, A., and Martin, M. A. (1986) *J. Virol.* **59**, 284–291
71. Milligan, J. F., Groebe, D. R., Witherell, G. W., and Uhlenbeck, O. C. (1987) *Nucleic Acids Res.* **15**, 8783–8798
72. Guo, J., Wu, W., Yuan, Z. Y., Post, K., Crouch, R. J., and Levin, J. G. (1995) *Biochemistry* **34**, 5018–5029
73. Drew, H. R. (1984) *J. Mol. Biol.* **176**, 535–557
74. SantaLucia, J., Jr. (1998) *Proc. Natl. Acad. Sci. U. S. A.* **95**, 1460–1465
75. Zuker, M., Mathews, D. H., and Turner, D. H. (1999) in *RNA Biochemistry and Biotechnology* (Barciszewski, J., and Clark, B. F. C., eds) pp. 11–43, Kluwer Academic Publishers Group, Dordrecht, The Netherlands
76. Mathews, D. H., Sabina, J., Zuker, M., and Turner, D. H. (1999) *J. Mol. Biol.* **288**, 911–940
77. Berkhout, B., van Wamel, J., and Klaver, B. (1995) *J. Mol. Biol.* **252**, 59–69
78. Dang, Q., and Hu, W.-S. (2001) *J. Virol.* **75**, 809–820
79. Pfeiffer, J. K., and Telesnitsky, A. (2001) *J. Virol.* **75**, 11263–11274
80. Roda, R. H., Balakrishnan, M., Kim, J. K., Roques, B. P., Fay, P. J., and Bambara, R. A. (2002) *J. Biol. Chem.* **277**, 46900–46911
81. Berkhout, B., Vastenhouw, N. L., Klasens, B. I. F., and Huthoff, H. (2001) *RNA* **7**, 1097–1114
82. Negroni, M., and Buc, H. (2000) *Proc. Natl. Acad. Sci. U. S. A.* **97**, 6385–6390
83. Moumen, A., Polomack, L., Unge, T., Véron, M., Buc, H., and Negroni, M. (2003) *J. Biol. Chem.* **278**, 15973–15982
84. Roda, R. H., Balakrishnan, M., Hanson, M. N., Wöhr, B. M., Le Grice, S. F. J., Roques, B. P., Gorelick, R. J., and Bambara, R. A. (2003) *J. Biol. Chem.* **278**, 31536–31546
85. South, T. L., and Summers, M. F. (1993) *Protein Sci.* **2**, 3–19
86. De Guzman, R. N., Wu, Z. R., Stalling, C. C., Pappalardo, L., Borer, P. N., and Summers, M. F. (1998) *Science* **279**, 384–388
87. Morellet, N., Déméné, H., Teilleux, V., Huynh-Dinh, T., de Rocquigny, H., Fournié-Zaluski, M.-C., and Roques, B. P. (1998) *J. Mol. Biol.* **283**, 419–434
88. Fisher, R. J., Rein, A., Fivash, M., Urbaneja, M. A., Casas-Finet, J. R., Medaglia, M., and Henderson, L. E. (1998) *J. Virol.* **72**, 1902–1909
89. Vuilleumier, C., Bombarda, E., Morellet, N., Gérard, D., Roques, B. P., and Mély, Y. (1999) *Biochemistry* **38**, 16816–16825
90. Berkhout, B., and Jeang, K.-T. (1991) *Nucleic Acids Res.* **19**, 6169–6176
91. Baudin, F., Marquet, R., Isel, C., Darlix, J.-L., Ehresmann, B., and Ehresmann, C. (1993) *J. Mol. Biol.* **229**, 382–397